Systematic variations in structural and electronic properties of BiFeO3 by A-site substitution

Zhang, Zhen; Wu, Ping; Chen, Lang; Wang, Junling

2010

Zhang, Z., Wu, P., Chen, L., & Wang, J. (2010). Systematic variations in structural and electronic properties of BiFeO3 by A-site substitution. Applied Physics Letters, 96.

https://hdl.handle.net/10356/99913

https://doi.org/10.1063/1.3279137

Systematic variations in structural and electronic properties of $BiFeO_3$ by A-site substitution

Zhen Zhang,[1] Ping Wu,[2] Lang Chen,[1] and Junling Wang[1,a)]
[1]*School of Materials Science and Engineering, Nanyang Technological University, Singapore 639798, Singapore*
[2]*Institute of High Performance Computing, 1 Science Park Road, #01-01 The Capricorn, Singapore 117528, Singapore*

(Received 20 October 2009; accepted 5 December 2009; published online 5 January 2010)

Systematic variations in the structural and electronic properties of $BiFeO_3$ with A-site substitutions were studied using first-principles density functional theory calculations. It is found that the ferroelectric distortion of $BiFeO_3$ with group IIIA element (Sc^{3+}, Y^{3+}, and La^{3+}) substitutions is significantly affected by the hybridization between substitute d states and oxygen 2*p* states, while that with group VB element (Sb^{3+}) substitution is stabilized by the s^2 lone pair electrons. For both groups, the substitute with smaller ionic size and larger electronegativity causes more significant off-center displacement and narrower band gap. © *2010 American Institute of Physics*. [doi:10.1063/1.3279137]

As the only known room temperature single-phase multiferroic material, $BiFeO_3$ is attractive for both fundamental research and applications.[1–5] However, $BiFeO_3$ suffers severe property deteriorations due to defects and nonstoichiometry such as secondary phases, cation vacancies, oxygen vacancies, and valence fluctuation of iron ions.[6–8] Chemical substitution is an effective way to improve the performance of $BiFeO_3$, and many substitutes have been studied experimentally.[9–12] Furthermore, chemical substitution could tailor the structural and electronic properties of $BiFeO_3$, and induce or enhance many interesting results, such as electrical modulation of conduction,[4] and hydrostatic-pressure-induced metal-insulator transition.[13]

In this work, we study the effects of A-site trivalent substitutes on the structural and electronic properties of $BiFeO_3$ using first-principles density functional theory calculations within the projector augmented wave (PAW) method implemented in the VASP.[14] The pseudopotential approach was adopted, where Bi $5d^{10}6s^26p^3$, Fe $3p^63d^64s^2$, and O $2s^22p^4$ orbitals were treated in the basis. The group IIIA elements Sc^{3+}, Y^{3+}, La^{3+}, and group VB element Sb^{3+} are considered as substitutes in this study, as their ionic radii are similar to that of Bi^{3+} (Table I).[15] For the substitutes, Sc $3s^23p^64s^23d^1$, Y $4s^24p^64d^15s^2$, La $5s^25p^65d^16s^2$, and Sb $5s^25p^3$ were considered as valence electrons. All calculations were performed with an energy cutoff of 500 eV for the plane wave expansion of the PAW, a $2\times2\times2$ Monkhorst Pack grid of k points, and the Fermi-smearing for the Brillouin zone integrations. We used the semiempirical LSDA+U method, where the strong Coulomb repulsion between localized d states is treated by adding a Hubbard-type term (U) to the effective potential, leading to a better description of the correlation effect in transition-metal oxides.[16] In this study, we used a value of U_{eff}=6 eV (U=6 eV and J=0 eV) in the framework of Dudarev's approach.[17,18]

A $2\times2\times2$ supercell was adopted for all the calculations, where the unit cell is consisted of two formula units. In view of the well-known deficiency of local density approximation (LDA) in calculating the lattice parameters of perovskite ferroelectrics,[19] we use experimental values of the unit cell (a=5.630, α=59.3°) for our calculations.[20] Rock-salt (G-type) antiferromagetic order with a homogeneous and collinear spin arrangement was used. To study the effects of A-site substitution, one of the Bi ions in the supercell is replaced with one substitute, corresponding to a doping concentration of 6.25%. All structures were relaxed while keeping the lat-

TABLE I. Calculated structural parameters (O–Fe–O bond angle, Fe–O–Fe bond angle, the shortest A–O and Fe–O bond length, and A–Fe distance), one-electron band-width, and energy band gaps for $BiFeO_3$ with A-site substitute. The coordination numbers for group VB and group IIIA substitutes are 6 and 9, respectively. The number in the brackets in the d_{A-Fe} row indicates the larger A–Fe distance. The number in the bracket for the ionic radius of Bi indicates that with a coordination number of 9.

	Group VB		Group IIIA		
Substitute	Sb	Bi	Sc	Y	La
Ionic radius	0.76	1.03(1.24)	0.92	1.08	1.21
Electronegativity	2.05	2.02	1.36	1.22	1.10
θ_{O-Fe-O} (deg)	162.5	166.4	165.7	168.7	171.1
$\theta_{Fe-O-Fe}$(deg)	157.7	155.6	152.2	154.4	157.0
d_{A-O} (Å)	2.10	2.29	2.13	2.33	2.52
d_{Fe-O} (Å)	1.92	1.96	1.95	1.95	1.96
d_{A-Fe} (Å)	2.93(4.03)	3.05(3.88)	2.88(4.08)	3.06(3.87)	3.23(3.65)
W (arb. units)	10.00	9.25	9.43	9.37	9.30
Band gap (eV)	2.28	2.45	2.34	2.39	2.42

a)Author to whom correspondence should be addressed. Electronic mail: jlwang@ntu.edu.sg.

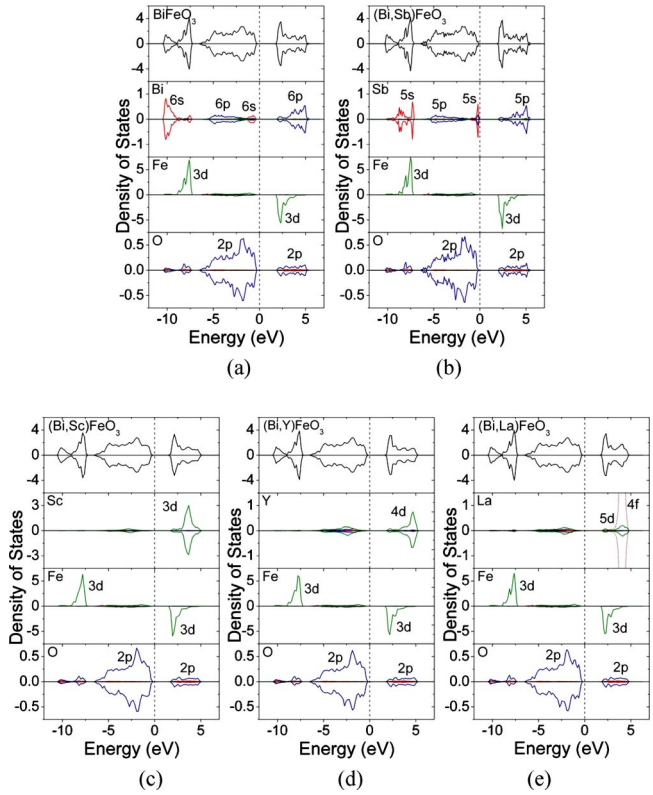

FIG. 1. (Color online) Calculated densities of states (DOS) for (a) pure $BiFeO_3$, and that with A-site substitute (b) Sb, (c) Sc, (d) Y, and (e) La. The panels from top to bottom show the total DOS, the partial substitutes DOS, partial Fe and O DOS for both spin channels calculated using the LSDA +U method with U_{eff}=6 eV, respectively. The zero is set to the calculated Fermi level.

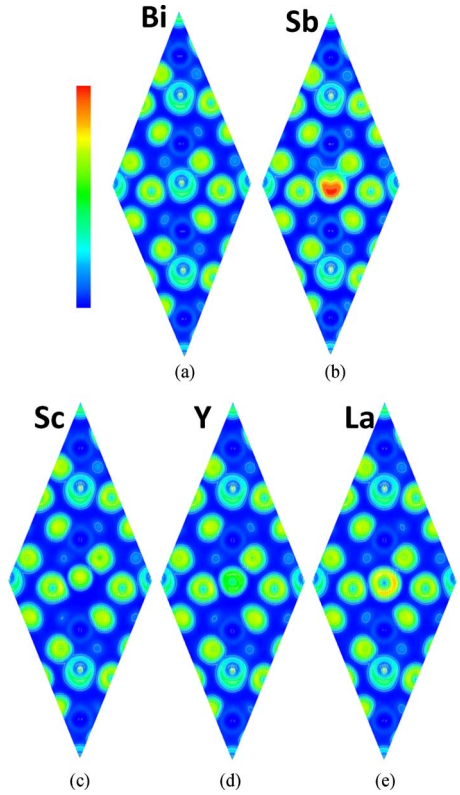

FIG. 2. (Color online) Valence ELF plots projected along the polar [111] axis [$(11\bar{2})$ plane] in (a) pure $BiFeO_3$, (b) Sb, (c) Sc, (d) Y, and (e) La-substituted $BiFeO_3$. The vertical middle axis follows the order of Bi–Fe–Bi–Fe–Substitute(Bi)–Fe–Bi–Fe–Bi. The upper end of the scale indicates no localization, and the bottom end corresponds to complete localization.

tice parameters fixed until the Hellman–Feynman forces are less than 10 meV/Å. The electronic structures were also analyzed by electron localization function (ELF), which provides a measure of the local influence of Pauli repulsion on the behavior of electrons and permits the mapping in real space of core, bonding, and nonbonding regions in a crystal.[21]

The calculated density of states (DOS) and partial DOS for both spin channels of $BiFeO_3$ [Fig. 1(a)] shows that the Fe 3*d*, Bi 6*p*/6*s*, and O 2*p* states are present in both conduction band and valence band, indicating both Bi–O and Fe–O bonding. The Bi $6s^2$ lone pair forms a space-filling localized lobe as shown in the ELF plot –[Fig. 2(a)], as a result of the mixing of Bi 6*p* states into the filled antibonding O 2*p* and Bi 6*s* states as proposed by Watson *et al.*[22] The anisotropic nature of the lone pair lobe causes the relative movements of Bi and Fe ions in the [111] direction leading to the giant ferroelectricity of $BiFeO_3$. And our calculation shows two different Bi–Fe distances of 3.05 and 3.87 Å along the threefold axis (Table I). All the calculated structural parameters, DOS and ELF plot of pure $BiFeO_3$ are in good agreement with the available data from experimental and other theoretical studies.[17,23–25]

In the Sb-substituted $BiFeO_3$, the lobelike Sb^{3+} $5s^2$ lone pair is also present. Moreover, Sb^{3+} $5s^2$ lone pair induces a greater localization than Bi^{3+} $6s^2$ lone pair, as shown in the ELF plot [Fig. 2(b)]. The more stereochemically active Sb^{3+} $5s^2$ lone pair lobe stabilizes a more distorted structure around Sb^{3+} ion. Our calculation shows a shorter Sb–Fe distance (2.93 Å) on one side, compared with 3.05 Å for Bi–Fe, and a longer distance on the other side (from 3.88 to 4.03 Å). Collectively, Sb–O bond is shortened to 2.10 Å, compared with Bi–O bond of 2.29 Å (Note that we only discuss the shortest A–O and Fe–O bond as they largely determine the properties of $BiFeO_3$). This structural shift could be explained by the stronger hybridization between Sb 5*s*/5*p* orbitals and O 2*p* orbitals than that between Bi 6*s*/6*p* and O 2*p* orbitals [Fig. 1(b)]; and hence the stereochemical activity of the Sb lone pair is stronger.[22]

In the La-substituted $BiFeO_3$, the local lattice around La^{3+} ion is close to a centrosymmetric structure without significant ferroelectric distortion, which is also in agreement with experimental observations.[12,26] In a clear contrast to Bi^{3+} and Sb^{3+} ions, La^{3+} ion shows a resistance to displacement from its centrosymmetric position, resulting in a longer La–Fe distance (3.23 Å) along the [111] direction and a lengthened La–O bond (2.52 Å). This effect could be explained by the turning-off of the stereochemically active lone pairs, as La^{3+} and Bi^{3+} have similar ionic sizes (1.21 and 1.24 Å, respectively).

However, it is striking to find that with reduced atomic number of the group IIIA substitutes (Sc^{3+} and Y^{3+}), the off-center displacement leading to ferroelectricity becomes more significant again. With the ionic radius shrinking from 1.21 Å (La) to 0.92 Å (Sc), A–Fe distance is shortened dramatically from 3.23 Å (La–Fe) to 3.06 Å (Y–Fe) and 2.88 Å (Sc–Fe) on one side, and lengthened from 3.65 to 3.87 Å and 4.08 Å on the other side. It is interesting to see that while the distortion of Y^{3+} is similar to that of Bi^{3+}, the off-center displacement of Sc^{3+} is even larger, giving rise to a stronger ferroelectricity. These considerable off-center displacements

do not originate from the localized electron lobes, as the ELF plots in Figs. 2(c)–2(e) show that the localized electrons around the group IIIA ions are nearly spherically distributed. On the other hand, the partial DOS analysis shown in Figs. 1(c)–1(e) indicate that Sc 3*d*, Y 4*d*, and La 5*d* states are present in the conduction band from 3.0 to 5.5 eV above the Fermi level as well as in the whole valence band, overlapping with O 2*p* states; and the overlapping increases as the atomic number decreases, indicating stronger A–O covalent bond. This trend could be explained by the increasing electronegativity of the cation increases (1.10 for La, 1.22 for Y, and 1.36 for Sc). Furthermore, the reduced substitute size with smaller atomic number makes ionic displacement structurally easier. Therefore we conclude that small ionic size and large electronegativity of the group IIIA substitute could cause significant displacement along [111] direction even without lobelike lone pair electrons.

Our calculations also reveal that the energy band gap of $BiFeO_3$ is reduced with smaller atomic number of both group IIIA and group VB trivalent A-site substitutes. For group VB elements, Sb substitution reduces the band gap to 2.28 from 2.45 eV of pure $BiFeO_3$. For group IIIA elements, with the reduced atomic number of substitute, the band gap decreases from 2.42 to 2.39 eV and 2.34 eV for La, Y, and Sc, respectively. This systematic variation of the electronic structure in $BiFeO_3$ by chemical substitutions could be explained by the Fe–O–Fe super-transfer mechanism where Fe 3*d* electron transfer is mediated by the O 2*p* states rather than the direct transfer between the 3*d* states. The one-electron bandwidth (W) depends on both the Fe–O–Fe bond angle and Fe–O bond length, through the overlap integrals between the Fe 3*d* orbitals and the O 2*p* orbitals. Proposed from tight-binding approximation, this double dependence could be described by the empirical formula $W \propto \cos\omega / d_{\mathrm{Fe-O}}^{3.5}$, where $\omega = 1/2(\pi - \langle \mathrm{Fe-O-Fe} \rangle)$.[27,28] In $BiFeO_3$, ω is the tilting angle, $\langle \mathrm{Fe-O-Fe} \rangle$ is Fe–O–Fe bond angle, and $d_{\mathrm{Fe-O}}$ is Fe–O bond length. As shown in Table I, for group VB elements, Sb substitute increases the Fe–O–Fe bond angle from 155.6° to 157.7°, and shortens the Fe–O bond from 1.96 to 1.94 Å. For group IIIA elements, Fe–O–Fe bond angle decreases from 157.0° (La), 154.4° (Y), and 152.2° (Sc), and the Fe–O bond length is reduced from 1.96 Å (La) to 1.95 Å (Y and Sc). All these structural changes result in a net increase of one-electron bandwidth (W). Therefore, substitution by smaller A-site cation than Bi leads a systematic reduction of band gap.

Moreover, the A–O hybridizations as well as Fe–O–Fe super-transfer mechanism may also contribute to the systematic variations in energy band gap by the substitutions, as both Fe 3*d* states and A-site cation states appear in the valence band and conduction band. For group VB element substitution, Sb–O bond length decreases by almost 10%. Similarly, significant shortening of A–O bonds is observed with decreasing atomic number of group IIIA substitutes. The shorter bond length indicates a stronger A–O hybridization and is also likely to induce a wider band dispersion and smaller band gap.

In summary, our theoretical study reveals that Sb^{3+} substituted $BiFeO_3$ has a larger ferroelectric distortion than pure $BiFeO_3$, as strong Sb–O hybridizations lead to a greater stereochemical activity of the Sb lone pair. On the contrary, La^{3+} substitution weakens the ferroelectricity in $BiFeO_3$ due to the fact the electrons localized at La site are spherically distributed. For other group IIIA elements (Sc^{3+}, Y^{3+}), it is striking to find that these substitutes could also lead to significant ferroelectric distortion. This off-center displacement is attributable to the small ionic size and large electronegativity of Sc^{3+} and Y^{3+}, leading to strong Sc–O and Y–O hybridization. The systematic change of band gap of $BiFeO_3$ with atomic number of group IIIA and group VB substitutes is closely related to Fe–O–Fe super-transfer and A–O hybridization as well.

The authors acknowledge the fruitful discussions with Professor Lu Li from National University of Singapore, and the support from Nanyang Technological University and Ministry of Education of Singapore under Projects Nos. AcRF RG30/06 and ARC 16/08.

[1] J. Wang, J. B. Neaton, H. Zheng, V. Nagarajan, S. B. Ogale, B. Liu, D. Viehland, V. Vaithyanathan, D. G. Schlom, U. V. Waghmare, N. A. Spaldin, K. M. Rabe, M. Wuttig, and R. Ramesh, Science **299**, 1719 (2003).
[2] W. Eerenstein, N. D. Mathur, and J. F. Scott, Nature (London) **442**, 759 (2006).
[3] J. Seidel, L.W. Martin, Q. He, Q. Zhan, Y.H. Chu, A. Rother, M.E. Hawkridge, P. Maksymovych, P. Yu, and M. Gajek, Nature Mater. **8**, 229 (2009).
[4] C. H. Yang, J. Seidel, S. Y. Kim, P. B. Rossen, P. Yu, M. Gajek, Y. H. Chu, L. W. Martin, M. B. Holcomb, and Q. He, Nature Mater. **8**, 485 (2009).
[5] G. Catalan and J. F. Scott, Adv. Mater. **21**, 2463 (2009).
[6] S. H. Lim, M. Murakami, W. L. Sarney, S. Q. Ren, A. Varatharajan, V. Nagarajan, S. Fujino, M. Wuttig, I. Takeuchi, and L. G. Salamanca-Riba, Adv. Funct. Mater. **17**, 2594 (2007).
[7] M. Murakami, S. Fujino, S. H. Lim, L. G. Salamanca-Riba, M. Wuttig, I. Takeuchi, V. Bindhu, H. Sugaya, T. Hasegawa, and S. E. Lofland, Appl. Phys. Lett. **88**, 112505 (2006).
[8] C. Ederer and N. A. Spaldin, Phys. Rev. B **71**, 224103 (2005).
[9] X. D. Qi, J. Dho, R. Tomov, M. G. Blamire, and J. L. MacManus-Driscoll, Appl. Phys. Lett. **86**, 062903 (2005).
[10] J. K. Kim, S. S. Kim, W. J. Kim, A. S. Bhalla, and R. Guo, Appl. Phys. Lett. **88**, 132901 (2006).
[11] Y. H. Lee, J. M. Wu, and C. H. Lai, Appl. Phys. Lett. **88**, 042903 (2006).
[12] S. K. Singh and H. Ishiwara, Jpn. J. Appl. Phys., Part 1 **45**, 3194 (2006).
[13] A. G. Gavriliuk, V. V. Struzhkin, I. S. Lyubutin, S. G. Ovchinnikov, M. Y. Hu, and P. Chow, Phys. Rev. B **77**, 155112 (2008).
[14] G. Kresse and J. Furthmüller, Phys. Rev. B **54**, 11169 (1996).
[15] R. D. Shannon, Acta Crystallogr., Sect. A: Cryst. Phys., Diffr., Theor. Gen. Crystallogr. **32**, 751 (1976).
[16] V. I. Anisimov, F. Aryasetiawan, and A. I. Lichtenstein, J. Phys.: Condens. Matter **9**, 767 (1997).
[17] J. B. Neaton, C. Ederer, U. V. Waghmare, N. A. Spaldin, and K. M. Rabe, Phys. Rev. B **71**, 014113 (2005).
[18] H. M. Tütüncü and G. P. Srivastava, J. Appl. Phys. **103**, 083712 (2008).
[19] D. Vanderbilt, Curr. Opin. Solid State Mater. Sci. **2**, 701 (1997).
[20] F. Kubel and H. Schmid, Acta Crystallogr., Sect. B: Struct. Crystallogr. Cryst. Chem. **46**, 698 (1990).
[21] B. Silvi and A. Savin, Nature (London) **371**, 683 (1994).
[22] G. W. Watson, S. C. Parker, and G. Kresse, Phys. Rev. B **59**, 8481 (1999).
[23] T. Higuchi, Y.-S. Liu, P. Yao, P.-A. Glans, J. Guo, C. Chang, Z. Wu, W. Sakamoto, N. Itoh, T. Shimura, T. Yogo, and T. Hattori, Phys. Rev. B **78**, 085106 (2008).
[24] P. Ravindran, R. Vidya, A. Kjekshus, H. Fjellvåg, and O. Eriksson, Phys. Rev. B **74**, 224412 (2006).
[25] C. Ederer and N. A. Spaldin, Phys. Rev. B **71**, 060401 (2005).
[26] Y. Wang, R. Y. Zheng, C. H. Sim, and J. Wang, J. Appl. Phys. **105**, 016106 (2009).
[27] M. Medarde, J. Mesot, P. Lacorre, S. Rosenkranz, P. Fischer, and K. Gobrecht, Phys. Rev. B **52**, 9248 (1995).
[28] P. G. Radaelli, G. Iannone, M. Marezio, H. Y. Hwang, S. W. Cheong, J. D. Jorgensen, and D. N. Argyriou, Phys. Rev. B **56**, 8265 (1997).